

Enhanced Early Galaxy Formation in JWST from Axion Dark Matter?

Simeon Bird^a, Chia-Feng Chang^a, Yanou Cui^a, Daneng Yang^{a,b}

^a*Department of Physics and Astronomy, University of California, Riverside, CA 92521, USA*

^b*Purple Mountain Observatory, Chinese Academy of Sciences, Nanjing 210033, China*

Abstract

We demonstrate that enhanced early galaxy formation can generically arise in axion-like particle (ALP) dark matter (DM) models with a delayed onset of axion field oscillation. In these models, the formation of localized massive objects enhances structure formation, potentially addressing the excess recently observed by the James Webb Space Telescope (JWST), while remaining consistent with existing constraints. We identify viable parameter space with the ALP mass in the range of $10^{-22} \text{ eV} < m_a < 10^{-19} \text{ eV}$. In addition, we show that the ALP parameter regions of interest can lead to intriguing complementary signatures in the small scale structure of DM halos and existing experimental searches for ALPs.

1. Introduction

The standard Λ CDM cosmology makes firm predictions for the abundance of dark matter halos as a function of time. However, recent James Webb Space Telescope (JWST) observations have revealed what may be an unexpectedly large population of luminous galaxies at redshifts 10 and above [1, 2, 3, 4, 5, 6, 7]. In particular, Ref. [6] reported 25 spectroscopically confirmed galaxies at $z_{\text{spec}} = 8.61 - 13.20$, two of which have $M_{\text{UV}} < -19.8$ mag at $z > 11$. The reported number exceeds most predictions based on the Λ CDM cosmology, and may be the harbinger of new fundamental physics and/or lead to a new understanding of structure formation [8, 9, 10, 11, 12, 13, 14, 15].

These surprising JWST results have inspired many dedicated studies [16, 14, 15, 17, 18, 19]. Proposed explanations for the JWST excess include enhanced star formation, accelerated mass assembly, early or clustering dark energies, large scale-dependent non-Gaussianities, cosmic string loops, etc. [20, 21, 22, 23, 24, 25, 26, 27, 28, 29, 30]. While it is possible that the JWST excess could be explained within the Λ CDM framework, it still requires refinements in our understanding of star formation efficiency [20, 21, 21, 31]. Therefore, proposals based on new physics are strong contenders as alternative explanations, such as a population of highly massive compact objects [32, 27, 25, 26], which is the focus of this work. The presence of these objects enhances the matter power spectrum (MPS) with a shot-noise-like contribution up to a certain truncation scale [33]. This shot noise enhancement could then trigger higher star formation efficiency, particularly in the most massive halos and at earlier epochs [32, 20, 34]. To fully address the excess, however,

these objects must be extremely massive and contribute a substantial fraction to the total matter content in the universe (Ω_m) [27, 25, 26].

A well-motivated source of such heavy compact objects is oscillatons arising from theories of axion dark matter (DM) with delayed onset of field oscillations [35, 36, 37, 38]. Parametric resonance in these theories leads to the formation of oscillons [39, 40, 41, 42, 43, 44, 45, 46, 47, 37], which are localized long-lived objects that may either decay or persist until the present day. In most cases, these oscillons remain localized and become oscillatons [48, 49, 50] supported by gravity by $z \sim 10$ [51, 52, 53, 54, 55, 56, 57], with masses ranging from $10^{-12} M_\odot$ to $10^4 M_\odot$ [32, 58]. The mass of these oscillatons anti-correlates with the axion mass m_a . The m_a range favored by the JWST excess is $10^{-19} \text{ eV} < m_a < 10^{-16} \text{ eV}$ in the Standard Misalignment Mechanism (SMM) [27], yet further requires a larger star formation efficiency f_* than expected from low redshift astrophysics. However, this mass range is excluded by black hole super-radiance (BHSR) [59, 27, 60, 61, 62].

In this work, we show that models with delayed axion oscillation can open up a parameter space safe from the BHSR constraint with astrophysically plausible f_* . In particular, we reveal a large viable parameter region with $10^{-22} \text{ eV} < m_a < 10^{-19} \text{ eV}$ that can explain the JWST excess, while being consistent with relevant constraints such as from BHSR, Lyman- α forest, and stellar dynamics [63, 64, 65, 60, 61, 62]. Furthermore, we demonstrate that the same ALP models that address the JWST excess may yield complementary signals in a variety of current/future axion search experiments [66, 67, 68], and intriguingly have the potential to alleviate puzzling features found in the small-scale structure of DM halos [69, 70, 71]. In addition, we identify a parameter range that is consistent with existing Λ CDM predictions, which is worth exploration even if the current JWST excess resolves upon further investigations.

Email addresses: sbird@ucr.edu (Simeon Bird), chiafeng.chang@email.ucr.edu (Chia-Feng Chang), yanou.cui@ucr.edu (Yanou Cui), danengy@ucr.edu (Daneng Yang)

¹Authors listed in alphabetical order.

2. Oscillatons from delayed ALP oscillation

Oscillatons are bound objects of a real scalar field (such as an ALP) sustained by self-interaction and gravity [35, 36, 37, 38]. They are commonly referred to as oscillons when the effect of gravity is negligible [39, 40, 41, 42, 43, 44, 45, 46, 72, 47, 37]. Since real scalar fields do not possess a conserved charge, the associated oscillons have a finite lifetime and can decay within the age of the universe. Nevertheless, an approximate $U(1)$ symmetry that appears in the non-relativistic regime makes them relatively long-lived [45, 72, 73, 47, 48]. Once they survive into the matter-dominated era, the effect of gravity may further stabilize their configurations, enabling them to persist until the present day [50, 47, 37].

ALP is one of the most well-motivated examples of a real scalar field due to its connections to QCD axions and string theories. Axions are pseudo-Nambu-Goldstone bosons arising from spontaneous breaking of global Peccei-Quinn (PQ) symmetries, originally proposed to solve the strong CP problem in QCD [74, 75, 76]. Later on, they were found to be attractive dark matter candidates, and more general non-QCD ALPs are also well motivated from theoretical frameworks such as string theory and supersymmetry [77, 78, 79, 80]. The very light m_a needed to affect high redshift structure growth as we found is incompatible with the QCD axion, but is generic for ALPs.

Axions can be produced from both misalignment mechanisms (MM) and the decay of axion topological defects. The axion energy density resulting from the latter mechanism is contingent upon model specifics and still under development, with uncertainties in part due to technical challenges in simulations (see e.g. [81, 82, 83, 84, 85, 86, 87, 88], and the refs therein). In particular, the effect of topological defects can be absent in certain cosmological scenarios. For example, if PQ symmetry breaking occurs before inflation, axion cosmic strings would be sufficiently diluted; on the other hand, the contribution from axion domain walls can be inconsequential when compared to that from the MM mechanism, if the lifetime of domain walls is sufficiently short. For these reasons, here we choose to focus on the formation of oscillatons via the misalignment mechanism.

In the standard misalignment mechanism (SMM), the axion field is initially displaced from its true potential minimum with zero initial velocity. It starts to oscillate when it acquires a mass m_a similar to the Hubble rate, $H_* \sim m_a$. There is no oscillon formation, and the coherent oscillations of the axion field contribute to the relic abundance of cold dark matter (CDM) today (Ω_a).

In contrast, when oscillons are formed, they typically arise from a delayed onset of ALP oscillations with parametric resonances. Our analysis assumes a significant delay in the onset of these oscillations and the subsequent formation of long-lived oscillons that persist until the present time. However, the specific model details leading to this scenario do not change our results.

Several mechanisms delaying the onset of ALP field oscillations have been investigated in the literature. For example, the ALP field may initially slow-roll in a plateau potential, remaining homogeneous until it reaches a deeper potential at later times. Such plateau potentials have been investigated in models motivated by α attractors and axion monodromy [35, 36, 37, 38, 47]. Alternatively, the initial field velocity is another approach to delay the onset of oscillation and has been explored in the context of kinetic misalignment (KMM) [89, 90]. In these models, oscillons also arise from parametric resonances. We will elaborate on such models with simulations in a forthcoming paper [91]. Meanwhile, several other models following analogous spirits have been explored in the literature such as large misalignment [92], trapped misalignment [93, 94], and KMM with radial excitations [95, 89, 96]. They all lead to some amount of delayed oscillations but do not span a large enough parameter space to enable all the DM energy density to go into oscillatons.

In this study, we focus on model-independent aspects of the delayed onset of oscillations and elaborate on its implications for JWST observations. The generic features are largely determined by two physical parameters: the mass of the ALP particle m_a and a dimensionless time parameter $\eta \equiv m_a/H_*$, which quantifies the degree of oscillation delay. A delayed oscillation corresponds to a larger value of η , compared to approximately 3 in the SMM. The fraction of the field that fragments saturate quickly with increasing η . To ensure that the ALP field is fully fragmented and forms oscillons, we focus on the parameter space where $\eta > 40$.

While η and f_a are in principle independent model parameters, for a given model with m_a and Ω_a specified, they have a 1 – 1 relation. As an example, for a simple, temperature-independent axion potential as used in most ALP models, f_a relates to η in the following way [97]:

$$f_a \approx 10^{15} \text{ GeV} \left(\frac{10^{-20} \text{ eV}}{m_a} \right)^{\frac{1}{4}} \left(\frac{90}{\eta} \right)^{\frac{3}{4}} \left(\frac{g_*}{4} \frac{\Omega_a h^2}{0.12} \right)^{\frac{1}{2}}, \quad (1)$$

where g_* is the effective degrees of freedom in the entropy evaluated at the onset of fragmentation. Throughout our paper, we will assume that all the DM is comprised of the oscillatons, i.e. $\Omega_a = \Omega_{\text{DM}}$, to fix η , which then fixes the 1 – 1 correspondence between f_a and η for a given m_a .

The main features of the oscillatons can be specified given the m_a and η parameters. Their mean separation can be determined by the comoving scale $d_{\text{osc}} = \pi/k_{\text{osc}}$, where $k_{\text{osc}} \approx m_a a_* \kappa_p$, with a_* being the scale factor at the onset of oscillation and $\kappa_p \sim O(1)$ a correction factor that we will specify later in Eq. (8) to incorporate a mild η dependence. The typical mass of the oscillaton can be estimated as

$$\begin{aligned} M_0 &\approx \bar{\rho}_a \frac{4\pi}{3} \left(\frac{\pi}{m_a a_* \kappa_p} \right)^3 \\ &\approx 10^4 M_\odot \left(\frac{70}{\eta} \right)^{\frac{3}{2} + 0.66 \theta(\eta - 80)} \left(\frac{4 \times 10^{-20} \text{ eV}}{m_a} \right)^{\frac{3}{2}}, \end{aligned} \quad (2)$$

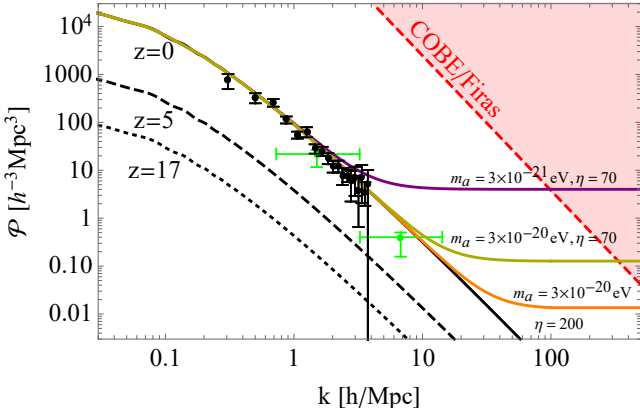


Figure 1: Example MPSs in delayed ALP oscillation models (colored curves) compared to the MPS from a standard Λ CDM model. Data points with error bars represent Lyman- α measurements (black) from Ref.[63] and HST UV luminosity function measurements (green) from Ref.[118]. The red dashed curve denotes the maximal cut-off scale for k^4 growth in the adiabatic curvature power spectrum based on the COBE/FIRAS bound from Ref.[119]. Higher resolution Lyman- α surveys can extend the scales on which the power spectrum is measured to $k \sim 10$ h/Mpc, similar to the UV luminosity data [34, 120].

where θ is the Heaviside Function, $\bar{\rho}_a$ is the average axion energy density and is taken to be the average DM energy density today. Both η and m_a anti-correlate with M_0 , i.e. M_0 decreases as η, m_a increases. For a fixed M_0 , increasing η can accommodate a smaller m_a , which can help alleviate the BHSR constraints. These axion clusters are produced from the collapse of the axion fields that fragmented at subhorizon scales.

The substantial mass of oscillatons naturally induces significant velocity dependent gravitational scatterings [98]. In terms of the oscillaton mass, we have

$$\frac{\sigma}{M_0} \approx 10 \text{ cm}^2/\text{g} \left(\frac{M_0}{10^4 M_\odot} \right) \left(\frac{10 \text{ km/s}}{v} \right)^4, \quad (3)$$

where v is the relative velocity between the two oscillatons and anomalies in DM small scale structure observations may be addressed by values of $O(1)$ cm^2/g [69, 70, 71, 99, 100, 101, 102, 103, 104, 105, 106, 107, 108, 109, 110, 111]. The wave nature of ALPs in our considered mass range gives rise to pc to kpc scale solitonic cores in ALP halos, which may also help alleviate small scale challenges in Λ CDM [112, 40, 55]. Given a large cross section, e.g., $10 \text{ cm}^2/\text{g}$, close encounters between oscillatons can merge them into larger, more diffuse structures within the ALP halos, enriching the small scale features of our model. The diffuse nature of the oscillatons also alleviates the existing stringent constraints from stellar dynamical, microlensing, and small-scale structures that apply to massive compact halo objects such as primordial black holes [64, 65, 113, 114, 115, 116, 117].

3. Matter power spectrum

We decomposed the density perturbation into linear and quadratic components following the methodology outlined in

Ref. [97]. The linear component approximately corresponds to the adiabatic perturbation in Λ CDM cosmology, denoted as $\mathcal{P}_{\text{CDM}}(k)$. On the other hand, the quadratic component introduces a shot noise-like contribution referred to as $\mathcal{P}_{\text{osc}}(k)$ which can be estimated as [26, 121, 122, 123]

$$\mathcal{P}_{\text{osc}}(k) \approx (D_{\text{iso}}(0) - 1)^2 \frac{f_{\text{osc}} M_0}{\rho_c \Omega_a} \propto M_0, \text{ for } k < k_{\text{osc}}. \quad (4)$$

Here ρ_c is the critical energy density today, f_{osc} is the fraction of dark matter comprised by oscillatons which we fix to be 1, $f_{\text{osc}} \rho_c \Omega_a / M_0$ is the number density of the oscillatons, and $D_{\text{iso}}(z)$ is the growth factor of isocurvature perturbations which can be parameterized as [122, 121, 123]

$$D_{\text{iso}}(z) = \left(1 + \frac{\Omega_a}{\Omega_m a_-} \frac{3a}{2a_{\text{eq}}} \right)^{a_-}, \quad (5)$$

where

$$a_- = (\sqrt{1 + 24\Omega_a/\Omega_m} - 1)/4. \quad (6)$$

The D_{iso} does not evolve at $a \ll a_{\text{eq}}$ and grow as $3a/(2a_{\text{eq}})$ (identical to the adiabatic one) for $\Omega_a = \Omega_m$ at $a \gg a_{\text{eq}}$. If oscillatons comprise only a fraction of dark matter, then $f_{\text{osc}} < 1$, resulting in a smaller $\mathcal{P}_{\text{osc}}(k)$. Note that the oscillaton number density is independent of Ω_a because $M_0 \propto \Omega_a$. However, \mathcal{P}_{osc} decreases as Ω_a decreases through the D_{iso} in Eq. 5 and Eq. 4, resulting in fewer high-z massive galaxies.

We numerically calculate the leading order $\mathcal{P}_{\text{osc}}(k)$, including backreaction, following Eq. 4.11 in Ref. [97], and parameterize the obtained results as²:

$$\mathcal{P}_{\text{osc}}(k) = \frac{2\pi^2}{k^3} \frac{f(\eta)(D_{\text{iso}}(0) - 1)^2}{(D_{\text{iso}}(z_{\text{eq}}) - 1)^2} \left(\frac{\kappa}{\kappa_p(\eta)} \right)^3 \theta(\kappa_p - \kappa), \quad (7)$$

where $\kappa \equiv \frac{k}{m_a a_*}$, $\kappa_p(\eta)$ and $f(\eta)$ are numerical factors parameterized as

$$\kappa_p(\eta) \simeq \begin{cases} 0.9, & 40 \leq \eta \leq 80, \\ 0.9 \left(\frac{\eta}{80} \right)^{0.22}, & 80 < \eta \leq 10^3, \end{cases} \quad (8)$$

and

$$f(\eta) \simeq 1.19 \left(\frac{\eta}{80} \right)^{-0.1}, \quad 40 < \eta \leq 10^3. \quad (9)$$

The spectrum $\mathcal{P}_{\text{osc}}(k)$ becomes dominant at scales larger than $k_* \approx a_* H_*$ and is truncated at k_{osc} . For $k > k_{\text{osc}}$, the spectrum becomes negligibly small and decreases as $1/k^2$ [97, 124].

In Fig. 1, we show the MPS for three benchmark examples. The M_0 is 1.6×10^3 , 1.5×10^4 M_\odot , and 4.9×10^5 for the orange, golden, and magenta cases, respectively. We will show in Fig. 3 that the case in gold color is favored in order to

²We solved for the relic abundance neglecting the effect of fragmentation which could induce a sub-O(1) uncertainty [124]. A more accurate determination of the relic abundance requires dedicated study which is beyond the scope of this work.

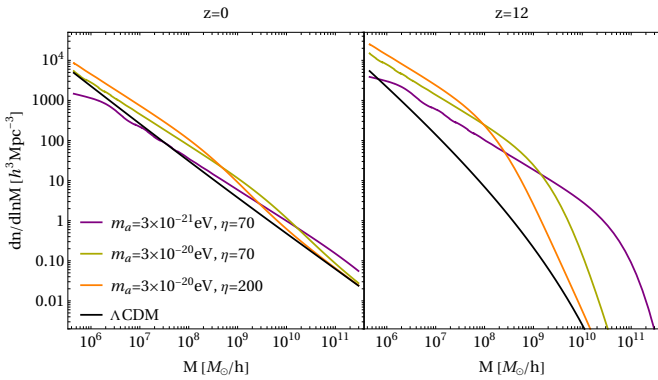


Figure 2: The halo mass function for the benchmark cases of Fig. 1 at redshifts $z = 0$ and $z = 12$.

explain the JWST excess, the orange case is consistent with ΛCDM , while the magenta case overproduces structures and is excluded by measurements of the UV luminosity function. In all cases, $\mathcal{P}_{\text{osc}}(k) \gg \mathcal{P}_{\text{CDM}}(k)$ for $k > k_*$, where the spectrum plateaus, before being truncated at $k \sim k_{\text{osc}}$ (beyond the range of Fig. 1). The case in gold color, specifically, has a transition around $k_* \sim 10 \text{ h/Mpc}$, which is close to the scale associated with the JWST excess.

4. Halo Mass Function

The clustering of oscillatons in the matter era leads to the formation of halos. We use the Press-Schechter formalism to estimate the halo mass function (HMF) from the MPS [125]. Given an MPS $\mathcal{P}(k)$ at redshift zero, we compute the mass variance using a top-hat window function as

$$\sigma_M^2(R) = \frac{1}{2\pi^2} \int dk \mathcal{P}(k) \left(3 \frac{\sin(kR) - kR \cos(kR)}{kR} \right)^2 k^2,$$

where M and R are halo mass and radius and are related through $M = 4\pi\bar{\rho}_m R^3/3$, with ρ_m being the mean matter density today, and the redshift dependence of σ_M is conventionally absorbed into the definition of $\delta_c(z)$. The HMF is computed in terms of $\nu \equiv \delta_c^2(z)/\sigma_M^2$ as

$$\frac{dn}{dM} = \frac{\bar{\rho}_m}{M} \nu f_{\text{EPS}}(\nu) \frac{d \ln \nu}{d \ln M}, \quad (10)$$

where $\nu f_{\text{EPS}}(\nu)$ is a shape function including the effect of ellipsoidal collapse from Ref. [126]. This approach has been widely applied in the literature because of its simplicity. Ref. [25] demonstrated that this technique can produce reliable approximations of the N-body reconstructed HMFs, even in the presence of massive primordial black holes.

In Fig. 2, we show the obtained HMFs for the ΛCDM and the three benchmarks in Fig. 1 at $z = 0$ (left) and $z = 12$ (right). We see that the HMFs at $z = 0$ are relatively similar across all cases; however, at $z = 12$, the delayed oscillation cases exhibit

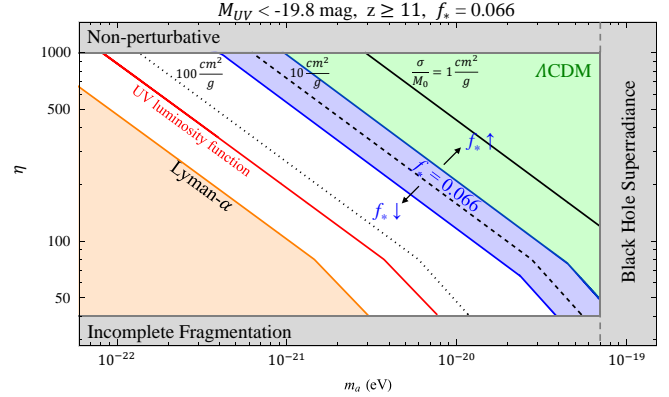


Figure 3: The viable model parameter space given the observations in Ref. [4], considering galaxies with $M_{\text{UV}} < -19.8$ mag at $z \geq 11$. The 68% CL preferred region shaded in blue corresponds to a prediction of $0.74 < N_{\text{exp}} < 4.3$. It is obtained for a star formation efficiency $f_* = 0.066$ and would shift up (down) if f_* increases (decreases). Black lines represent contours of the gravitational scattering cross section per mass for values of 1, 10, and $100 \text{ cm}^2/\text{g}$, evaluated at a velocity of $v = 10 \text{ km/s}$. At larger velocities, the cross section quickly reduces due to the v^{-4} dependence. Constraints from various sources exclude certain regions: the Lyman- α forest data [63] disfavors the orange area; the region to the left of the red curve is inconsistent with measured UV luminosity functions [118]; and the grey area to the right is excluded by BHSR constraints [59, 60, 61, 62].

significant enhancements towards larger halo masses, increasing the likelihood of finding halos hosting the very massive galaxies. Once small halos virialize, they almost decouple from the background evolution. Hence the abundance of massive halos is largely unaffected at low redshifts. As a result, the effect of our model becomes less significant today, which alleviates constraints from low redshift measurements [123, 117].

5. Parameter space favored by JWST excess

The enhanced massive halo population as we see in Fig. 2 can trigger earlier galaxy formation and enhance the formation efficiency [32, 20]. To convert the model prediction for HMF into the number of observed galaxies, we consider a simplified approach assuming a constant star formation efficiency f_* . We compute the expected number of observed galaxies with $M_{\text{UV}} < -19.8$ mag at $z > 11$ as considered in Fig. 13 of Ref. [6], where the number of observed galaxies $N_{\text{obs}} = 2$ is systematically higher than theoretical predictions from the literature [8, 9, 10, 11, 12, 13], e.g., 0.3 from Ref. [127] as a recent estimate. We convert the requirement of $M_{\text{UV}} < -19.8$ mag into a minimum halo mass by using the $M_* - M_{\text{UV}}$ relation of Ref. [127]. Assuming a constant star formation efficiency f_* , we set the minimum halo mass $M_{\text{min}} = 1.8 \times 10^9 e^{-0.12z_{\text{min}}/(f_* f_b)} M_\odot$, where $z_{\text{min}} = 11$, $f_b \approx 0.16$ is the baryon fraction in the matter energy density, and we set $f_* = 0.066$ so that the ΛCDM prediction is for an expected 0.3 galaxies at $z > 11$ [127]. The value of $f_* = 0.066$ is within expectations for a $10^{12} M_\odot$ halo at $z=0$, but small compared to some theoretical models proposed to explain the

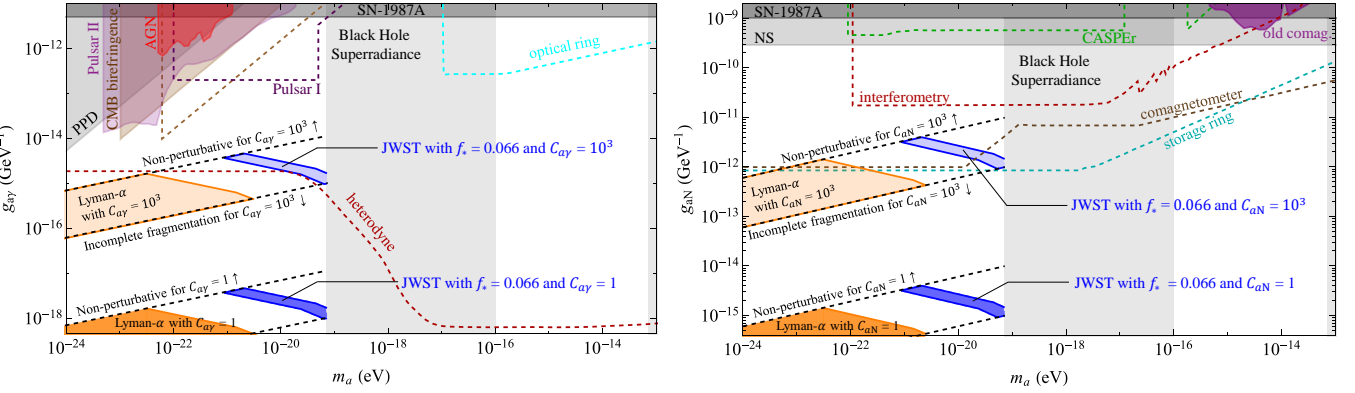


Figure 4: Axion-photon (left) and axion-nucleon (right) couplings versus axion DM mass m_a (assuming $\Omega_a = \Omega_{\text{DM}}$ in Eq. 1). The blue and the lighter-blue regions correspond to the regions favoured by matching the JWST excess, with $C_{ay,N} = 1$ and $C_{ay,N} = 10^3$, respectively. The blue regions are bounded by two dashed black lines, corresponding to the requirement of perturbative η with complete fragmentation. Constraints from various existing searches (solid shaded regions) and forecasts (colored dashed lines) are also illustrated. See text for further details.

JWST excess solely by extra star formation [20, 15, 14, 13, 128]. It has been noted that an excessively high f_* could introduce new tensions with the cosmic reionization history [129], making our obtained value a more desirable option. The number of expected galaxies count is calculated as

$$N_{\text{exp}} = \frac{A_{\text{eff}}}{4\pi} \int_{11}^{z_{\text{max}}} dz \frac{dV_c}{dz} \int_{M_{\text{min}}}^{M_{\text{max}}} dM \frac{dn}{dM}, \quad (11)$$

where $A_{\text{eff}} = 45 \text{ arcmin}^2$ is the effective area of the observation following Ref. [6] and V_c is the comoving Hubble volume at z . dn/dM is the HMF in Eq. 10. Our result is not sensitive to z_{max} , M_{max} , provided that they are sufficiently large.

Fig. 3 presents the preferred 68% CL parameter regions for a constant $f_* = 0.066$ as a blue band in the $m_a - \eta$ plane. We obtain the blue band considering $0.74 < N_{\text{exp}} < 4.3$ which arises from a Feldman-Cousins analysis for two observations and zero background [130], and the lower limit happens to coincide with that from Ref. [6]. For a higher (lower) value of f_* , the band would shift upward (downward). The upper-right corner corresponds to lower prediction for N_{exp} values that are consistent with ΛCDM predictions within the uncertainties [8, 9, 10, 11, 12, 13]. The lower-left region has higher N_{exp} and is constrained by Lyman- α and UV luminosity measurements [63, 118]. We also plot the contours of the gravitational scattering cross section of Eq. (3) evaluated at $v = 10 \text{ km/s}$ in Fig. 3. In the viable region, we see that the gravitational cross section takes values in $(1 - 100) \text{ cm}^2/\text{g}$, which could lead to novel signal predictions that can address the small-scale observations, e.g., the core-cusp problem and the too-big-to-fail problem [69, 70, 71, 99, 100, 101, 102, 103, 104, 105, 106, 107, 108, 109, 110, 111].

6. Implications for Axion Models and Complementary Searches

As shown in the last section, axion models with delayed ALP oscillations can address the JWST excess, with a

preferred parameter space spanning $4 \times 10^{-22} \text{ eV} < m_a < 10^{-19} \text{ eV}$ and $40 < \eta < 1000$. Existing ALP searches may provide valuable complementary probes for such ALPs, albeit in a model-dependent way. While the impact of ALP on structure formation is largely independent of the non-gravitational axion coupling to the Standard Model (SM) particles, most other ALP searches do depend on the specific coupling patterns. Here we focus on axion interactions with photons and nucleons (N), as described by

$$\mathcal{L} \in \frac{g_{ay}}{4} a F_{\mu\nu} \tilde{F}^{\mu\nu} + g_{aN} \partial_\mu a \bar{N} \gamma^\mu \gamma^5 N, \quad (12)$$

with effective couplings

$$g_{ay} = C_{ay} \alpha / (2\pi f_a), \quad g_{aN} = C_{aN} / f_a, \quad (13)$$

where $F_{\mu\nu}$ represents the electromagnetic field strength, and C_{ay} , C_{aN} are model-dependent parameters. In standard QCD axion inspired models such as KSVZ or DFSZ [131, 132, 133, 134], C_{ay} , $C_{aN} \sim O(1)$. Meanwhile, other recently proposed well-motivated axion theories such as those with multiple PQ fermions, vector kinetic mixing, and axion clockworks, can generically predict significantly larger coupling C 's, up to $O(10^2 - 10^3)$ [135, 136, 137]. According to Eqs. 1 and 13, with our assumption of $\Omega_a = \Omega_{\text{DM}}$, f_a and the corresponding η are fixed for given g_{ay} (g_{aN}) and C_{ay} (C_{aN}). Thus we may map the parameter regions in Fig. 3 onto the $m_a - g_{ay,N}$ space as in Fig. 4. In light of the aforementioned theoretically motivated range for C_{ay} , C_{aN} , in Fig. 4, the JWST excess favored regions are illustrated for two benchmark values: C_{ay} , $C_{aN} = 1$ (blue band) and C_{ay} , $C_{aN} = 1000$ (light blue band). The viable regions for other values of $1 \lesssim C_{ay}$, $C_{aN} \lesssim 1000$ are expected to lie between these two bands. These bands are truncated from above and below (denoted by dashed black lines) by requiring that the corresponding η are within the perturbative regime with complete fragmentation, $40 \lesssim \eta \lesssim 1000$ (see discussion above Eq. 1), which we have chosen to focus on in our analysis. As C_{ay} or C_{aN} increases, the blue and orange bands,

along with the black dashed lines, would linearly shift upwards. We also show the current constraints (solid shaded regions) and future sensitivity forecast (bounded above by colored dashed lines) for a variety of experiments/observations, including Lyman- α [63], BHSR [60, 61, 62], Supernova-1987A [138], neutron star cooling (NS) [139, 140, 141, 142], protoplanetary disk polarimetry (PPD) [143], active galactic nuclei (AGN) [144], and old comagnetometer [68].

As can be seen from Fig. 4, upcoming experiments can offer complementary probes for the parameter range that could address the JWST excess. For example, for the benchmark of $C_{ay} = 1000$ the reach of future heterodyne experiments [66] overlaps with the JWST excess favored region of (g_{ay}, m_a) . Similarly, future storage ring and comagnetometer experiments would be able to explore the (g_{aN}, m_a) range motivated by the JWST excess [67, 68]. It is also worth noting that the experiments covering the further upper regions in Fig. 4, such as interferometry [145] and linearly polarized pulsar light (Pulsar I in Fig. 4 left) [146], can potentially probe ALPs with $\eta > 10^3$ and C_{ay} (or C_{aN}) $> 10^3$. However, these regions require a non-perturbative analysis of fragmentation ($\eta \gtrsim 10^3$), which is beyond the scope of this study.

We note that in our preferred parameter range, the onset of delayed axion oscillation occurs at $T_* \lesssim 10$ keV. Such a late onset is potentially subject to constraint from Big Bang Nucleosynthesis (BBN) [124] if the dark sector induces a sufficiently large change in the energy density. For most mechanisms of realizing a delayed oscillation as outlined in Section 2, the effect on BBN is negligible, such as the α attractor and axion monodromy models that implement the delay through a long flat plateau region in the potential [35, 36, 37, 38]. A potentially notable impact on BBN would only occur in minimal KMM models without regulating the extrapolation of kinetic energy towards arbitrarily higher temperatures or earlier times [124]. However, in realistic models, the dominance of axion kinetic energy must be transient, initially preceded by the dominance of another form of energy, which may provide a natural cutoff to the kinetic energy domination and thus alleviate the BBN constraint. The results of this work is independent of such model specifics. We will elaborate related discussions based on specific models in a follow-up work [91]. In synergy with our study, recently there has been a general rising interest in viable post-BBN dark sector dynamics, which can lead to observable features in supermassive black holes, primordial gravitational waves, and small-scale structures, offering potential insights into recent astrophysical observations [147, 148, 149, 150, 151, 152, 153, 93, 27, 94, 154, 155].

7. Conclusion

We demonstrated that there is a large parameter space of axion dark matter with $10^{-22}\text{eV} \lesssim m_a \lesssim 10^{-19}\text{eV}$ that can address the JWST excess while being compatible with all existing constraints, in the framework where the axions

undergo a delayed oscillation. The delayed onset of the axion field oscillation allows for efficient axion field fragmentation at subhorizon scales. The fragmented axion field collapses into a large population of massive oscillations, which leads to more massive galaxies at high redshift, and thus can potentially address the excess observed by JWST. Upcoming experiments can provide complementary probes for the ALP parameter range favored by the JWST excess. Near-future Lyman- α forest surveys such as Weave-QSO [156] or DESI [157, 158] will extend the scales on which the MPS can be measured by a further factor of 2 – 3. Future surveys of strong lensing caustics could directly detect the predicted signature from small halos [159]. We also identified sizable gravitational scattering in our model parameter space, which enriches small scale structure formation in our model that is worth further investigation [70, 71]. In addition to the complementary astrophysical probes related to structure formation, we demonstrated that the JWST excess favored parameter region can be probed by existing or planned axion search avenues, e.g. heterodyne, comagnetometer and storage ring experiments, assuming certain patterns of ALP-SM couplings (i.e. fixed C_{ay} , C_{aN}). This study identifies new avenues for probing axion DM, and would stand as a worthwhile addition to the literature even if the current JWST excess resolves after further investigation.

8. Acknowledgment

We thank Yuichi Harikane, Huangyu Xiao, and Hai-Bo Yu for the helpful discussion. SB is supported by NASA ATP-80NSSC21K1840. CC and YC are supported by the US Department of Energy under award number DE-SC0008541. DY is supported by the John Templeton Foundation under grant ID #61884 and the U.S. Department of Energy under grant No. de-sc0008541. The opinions expressed in this publication are those of the authors and do not necessarily reflect the views of the John Templeton Foundation.

References

- [1] I. Labb , P. van Dokkum, E. Nelson, R. Bezanson, K. A. Suess, J. Leja, G. Brammer, K. Whitaker, E. Mathews, M. Stefanon, B. Wang, A population of red candidate massive galaxies 600 Myr after the Big Bang, *Nature* 616 (7956) (2023) 266–269. [arXiv:2207.12446](https://arxiv.org/abs/2207.12446), doi: [10.1038/s41586-023-05786-2](https://doi.org/10.1038/s41586-023-05786-2).
- [2] H. Atek, M. Shuntov, L. J. Furtak, J. Richard, J.-P. Kneib, G. Mahler, A. Zitrin, H. J. McCracken, S. Charlot, J. Chevallard, I. Chemerynska, Revealing galaxy candidates out to $z \sim 16$ with JWST observations of the lensing cluster SMACS0723, *Mon. Not. R. Astron. Soc.* 519 (1) (2023) 1201–1220. [arXiv:2207.12338](https://arxiv.org/abs/2207.12338), doi: [10.1093/mnras/stac3144](https://doi.org/10.1093/mnras/stac3144).
- [3] S. L. Finkelstein, M. B. Bagley, P. A. Haro, M. Dickinson, H. C. Ferguson, J. S. Kartaltepe, C. Papovich, D. Burgarella, D. D. Kocevski, M. Huertas-Company, K. G. Iyer, A. M. Koekemoer, R. L. Larson, P. G. P  rez-Gonz  lez, C. Rose, et al., A Long Time Ago in a Galaxy Far, Far Away: A Candidate $z \sim 12$ Galaxy in Early JWST CEERS Imaging, *Astrophys. J. Lett.* 940 (2) (2022) L55. [arXiv:2207.12474](https://arxiv.org/abs/2207.12474), doi: [10.3847/2041-8213/ac966e](https://doi.org/10.3847/2041-8213/ac966e).
- [4] Y. Harikane, M. Ouchi, M. Oguri, Y. Ono, K. Nakajima, Y. Isobe, H. Umeda, K. Mawatari, Y. Zhang, A Comprehensive Study of Galaxies at $z \sim 9$ –16 Found in the Early JWST Data: Ultraviolet Luminosity

- Functions and Cosmic Star Formation History at the Pre-reionization Epoch, *Astrophys. J. Suppl. Ser.* 265 (1) (2023) 5. [arXiv:2208.01612](https://arxiv.org/abs/2208.01612), doi:10.3847/1538-4365/acaaa9.
- [5] L. D. Bradley, D. Coe, G. Brammer, L. J. Furtak, R. L. Larson, F. Andrade-Santos, R. Bhatawdekar, M. Bradac, T. Broadhurst, A. Carnall, C. J. Conselice, J. M. Diego, B. Frye, S. Fujimoto, T. Y.-Y. Hsiao, et al., High-Redshift Galaxy Candidates at $z = 9 - 13$ as Revealed by JWST Observations of WHL0137-08, arXiv e-prints (Oct. 2022). [arXiv:2210.01777](https://arxiv.org/abs/2210.01777), doi:10.48550/arXiv.2210.01777.
- [6] Y. Harikane, K. Nakajima, M. Ouchi, H. Umeda, Y. Isobe, Y. Ono, Y. Xu, Y. Zhang, Pure Spectroscopic Constraints on UV Luminosity Functions and Cosmic Star Formation History From 25 Galaxies at $z_{\text{spec}} = 8.61 - 13.20$ Confirmed with JWST/NIRSpec, arXiv e-prints (Apr. 2023). [arXiv:2304.06658](https://arxiv.org/abs/2304.06658), doi:10.48550/arXiv.2304.06658.
- [7] J. P. Gardner, J. C. Mather, M. Clampin, R. Doyon, M. A. Greenhouse, H. B. Hammel, J. B. Hutchings, P. Jakobsen, S. J. Lilly, K. S. Long, J. I. Lunine, M. J. McCaughrean, M. Mountain, J. Nella, G. H. Rieke, et al., The James Webb Space Telescope, *Space Sci. Rev.* 123 (4) (2006) 485–606. [arXiv:astro-ph/0606175](https://arxiv.org/abs/astro-ph/0606175), doi:10.1007/s11214-006-8315-7.
- [8] P. Dayal, A. Ferrara, J. S. Dunlop, F. Pacucci, Essential physics of early galaxy formation, *Mon. Not. R. Astron. Soc.* 445 (3) (2014) 2545–2557. [arXiv:1405.4862](https://arxiv.org/abs/1405.4862), doi:10.1093/mnras/stu1848.
- [9] P. Dayal, E. M. Rossi, B. Shiralilou, O. Piana, T. R. Choudhury, M. Volonteri, The hierarchical assembly of galaxies and black holes in the first billion years: predictions for the era of gravitational wave astronomy, *Mon. Not. R. Astron. Soc.* 486 (2) (2019) 2336–2350. [arXiv:1810.11033](https://arxiv.org/abs/1810.11033), doi:10.1093/mnras/stz897.
- [10] L. Y. A. Yung, R. S. Somerville, S. L. Finkelstein, G. Popping, R. Davé, A. Venkatesan, P. Behroozi, H. C. Ferguson, Semi-analytic forecasts for JWST - IV. Implications for cosmic reionization and LyC escape fraction, *Mon. Not. R. Astron. Soc.* 496 (4) (2020) 4574–4592. [arXiv:2001.08751](https://arxiv.org/abs/2001.08751), doi:10.1093/mnras/staa1800.
- [11] P. Behroozi, C. Conroy, R. H. Wechsler, A. Hearin, C. C. Williams, B. P. Moster, L. Y. A. Yung, R. S. Somerville, S. Gottlöber, G. Yepes, R. Endsley, The Universe at $z > 10$: predictions for JWST from the UNIVERSEMACHINE DR1, *Mon. Not. R. Astron. Soc.* 499 (4) (2020) 5702–5718. [arXiv:2007.04988](https://arxiv.org/abs/2007.04988), doi:10.1093/mnras/staa3164.
- [12] S. M. Wilkins, A. P. Vijayan, C. C. Lovell, W. J. Roper, D. Irodotou, J. Caruana, L. T. C. Seeyave, J. K. Kuusisto, P. A. Thomas, S. A. K. Parris, First light and reionization epoch simulations (FLARES) V: the redshift frontier, *Mon. Not. R. Astron. Soc.* 519 (2) (2023) 3118–3128. [arXiv:2204.09431](https://arxiv.org/abs/2204.09431), doi:10.1093/mnras/stac3280.
- [13] C. A. Mason, M. Trenti, T. Treu, The brightest galaxies at cosmic dawn, *Mon. Not. R. Astron. Soc.* 521 (1) (2023) 497–503. [arXiv:2207.14808](https://arxiv.org/abs/2207.14808), doi:10.1093/mnras/stad035.
- [14] C. C. Lovell, I. Harrison, Y. Harikane, S. Tacchella, S. M. Wilkins, Extreme value statistics of the halo and stellar mass distributions at high redshift: are JWST results in tension with Λ CDM?, *Mon. Not. R. Astron. Soc.* 518 (2) (2023) 2511–2520. [arXiv:2208.10479](https://arxiv.org/abs/2208.10479), doi:10.1093/mnras/stac3224.
- [15] M. Boylan-Kolchin, Stress Testing Λ CDM with High-redshift Galaxy Candidates, arXiv e-prints (8 2022). [arXiv:2208.01611](https://arxiv.org/abs/2208.01611), doi:10.1038/s41550-023-01937-7.
- [16] N. Sabti, J. B. Muñoz, M. Kamionkowski, Insights from HST into Ultra-Massive Galaxies and Early-Universe Cosmology, arXiv e-prints (May 2023). [arXiv:2305.07049](https://arxiv.org/abs/2305.07049), doi:10.48550/arXiv.2305.07049.
- [17] Y. Chen, H. J. Mo, K. Wang, Massive Dark Matter Halos at High Redshift: Implications for Observations in the JWST Era, arXiv e-prints (4 2023). [arXiv:2304.13890](https://arxiv.org/abs/2304.13890).
- [18] J. McCaffrey, S. Hardin, J. Wise, J. Regan, No Tension: JWST Galaxies at $z > 10$ Consistent with Cosmological Simulations, arXiv e-prints (Apr. 2023). [arXiv:2304.13755](https://arxiv.org/abs/2304.13755), doi:10.48550/arXiv.2304.13755.
- [19] R. Kannan, V. Springel, L. Hernquist, R. Pakmor, A. M. Delgado, B. Hadzhiyska, C. Hernández-Aguayo, M. Barrera, F. Ferlito, S. Bose, S. White, C. Frenk, A. Smith, E. Garaldi, The MillenniumTNG Project: The galaxy population at $z \geq 8$, arXiv e-prints (Oct. 2022). [arXiv:2210.10066](https://arxiv.org/abs/2210.10066), doi:10.48550/arXiv.2210.10066.
- [20] A. Dekel, K. S. Sarkar, Y. Birnboim, N. Mandelker, Z. Li, Efficient Formation of Massive Galaxies at Cosmic Dawn by Feedback-Free Starbursts, arXiv e-prints (3 2023). [arXiv:2303.04827](https://arxiv.org/abs/2303.04827), doi:10.1093/mnras/stad1557.
- [21] G. Sun, C.-A. Faucher-Giguère, C. C. Hayward, X. Shen, A. Wetzel, R. K. Cochrane, Bursty Star Formation Naturally Explains the Abundance of Bright Galaxies at Cosmic Dawn, *Astrophys. J. Lett.* 955 (2) (2023) L35. [arXiv:2307.15305](https://arxiv.org/abs/2307.15305), doi:10.3847/2041-8213/acf85a.
- [22] E. O. Nadler, A. Benson, T. Driskell, X. Du, V. Gluscevic, Growing the first galaxies' merger trees, *Mon. Not. R. Astron. Soc.* 521 (3) (2023) 3201–3220. [arXiv:2212.08584](https://arxiv.org/abs/2212.08584), doi:10.1093/mnras/stad666.
- [23] S. Passaglia, M. Sasaki, Primordial black holes from CDM isocurvature perturbations, *Phys. Rev. D* 105 (10) (2022) 103530. [arXiv:2109.12824](https://arxiv.org/abs/2109.12824), doi:10.1103/PhysRevD.105.103530.
- [24] M. Biagetti, G. Franciolini, A. Riotto, High-redshift JWST Observations and Primordial Non-Gaussianity, *Astrophys. J.* 944 (2) (2023) 113. [arXiv:2210.04812](https://arxiv.org/abs/2210.04812), doi:10.3847/1538-4357/acb5ea.
- [25] B. Liu, S. Zhang, V. Bromm, Effects of stellar-mass primordial black holes on first star formation, *Mon. Not. Roy. Astron. Soc.* 514 (2) (2022) 2376–2396. [arXiv:2204.06330](https://arxiv.org/abs/2204.06330), doi:10.1093/mnras/stac1472.
- [26] B. Liu, V. Bromm, Accelerating Early Massive Galaxy Formation with Primordial Black Holes, *Astrophys. J. Lett.* 937 (2) (2022) L30. [arXiv:2208.13178](https://arxiv.org/abs/2208.13178), doi:10.3847/2041-8213/ac927f.
- [27] G. Hütsi, M. Raidal, J. Urutia, V. Vaskonen, H. Veermäe, Did JWST observe imprints of axion miniclusters or primordial black holes?, *Phys. Rev. D* 107 (4) (2023) 043502. [arXiv:2211.02651](https://arxiv.org/abs/2211.02651), doi:10.1103/PhysRevD.107.043502.
- [28] R. C. Batista, V. Marra, Clustering dark energy and halo abundances, *JCAP* 11 (2017) 048. [arXiv:1709.03420](https://arxiv.org/abs/1709.03420), doi:10.1088/1475-7516/2017/11/048.
- [29] A. Klypin, V. Poulin, F. Prada, J. Primack, M. Kamionkowski, V. Avila-Reese, A. Rodriguez-Puebla, P. Behroozi, D. Hellinger, T. L. Smith, Clustering and halo abundances in early dark energy cosmological models, *Mon. Not. R. Astron. Soc.* 504 (1) (2021) 769–781. [arXiv:2006.14910](https://arxiv.org/abs/2006.14910), doi:10.1093/mnras/stab769.
- [30] H. Jiao, R. Brandenberger, A. Refregier, Early Structure Formation from Cosmic String Loops in Light of Early JWST Observations, arXiv e-prints (4 2023). [arXiv:2304.06429](https://arxiv.org/abs/2304.06429).
- [31] M. Haslbauer, P. Kroupa, A. H. Zonoozi, H. Haghi, Has JWST Already Falsified Dark-matter-driven Galaxy Formation?, *Astrophys. J. Lett.* 939 (2) (2022) L31. [arXiv:2210.14915](https://arxiv.org/abs/2210.14915), doi:10.3847/2041-8213/ac9a50.
- [32] K. M. Zurek, C. J. Hogan, T. R. Quinn, Astrophysical Effects of Scalar Dark Matter Miniclusters, *Phys. Rev. D* 75 (2007) 043511. [arXiv:astro-ph/0607341](https://arxiv.org/abs/astro-ph/0607341), doi:10.1103/PhysRevD.75.043511.
- [33] B. Carr, J. Silk, Primordial Black Holes as Generators of Cosmic Structures, *Mon. Not. Roy. Astron. Soc.* 478 (3) (2018) 3756–3775. [arXiv:1801.00672](https://arxiv.org/abs/1801.00672), doi:10.1093/mnras/sty1204.
- [34] V. Iršič, H. Xiao, M. McQuinn, Early structure formation constraints on the ultralight axion in the postinflation scenario, *Phys. Rev. D* 101 (12) (2020) 123518. [arXiv:1911.11150](https://arxiv.org/abs/1911.11150), doi:10.1103/PhysRevD.101.123518.
- [35] J. Soda, Y. Urakawa, Cosmological imprints of string axions in plateau, *Eur. Phys. J. C* 78 (9) (2018) 779. [arXiv:1710.00305](https://arxiv.org/abs/1710.00305), doi:10.1140/epjc/s10052-018-6246-6.
- [36] N. Kitajima, J. Soda, Y. Urakawa, Gravitational wave forest from string axiverse, *JCAP* 10 (2018) 008. [arXiv:1807.07037](https://arxiv.org/abs/1807.07037), doi:10.1088/1475-7516/2018/10/008.
- [37] J. Ollé, O. Pujolàs, F. Rompineve, Oscillons and Dark Matter, *JCAP* 02 (2020) 006. [arXiv:1906.06352](https://arxiv.org/abs/1906.06352), doi:10.1088/1475-7516/2020/02/006.
- [38] P. Brax, J. A. R. Cembranos, P. Valageas, Nonrelativistic formation of scalar clumps as a candidate for dark matter, *Phys. Rev. D* 102 (8) (2020) 083012. [arXiv:2007.04638](https://arxiv.org/abs/2007.04638), doi:10.1103/PhysRevD.102.083012.
- [39] L. A. Urena-Lopez, Oscillations revisited, *Class. Quant. Grav.* 19 (2002) 2617–2632. [arXiv:gr-qc/0104093](https://arxiv.org/abs/gr-qc/0104093), doi:10.1088/0264-9381/19/10/307.
- [40] D. J. E. Marsh, Axion Cosmology, *Phys. Rept.* 643 (2016) 1–79. [arXiv:1510.07633](https://arxiv.org/abs/1510.07633), doi:10.1016/j.physrep.2016.06.005.
- [41] I. L. Bogolyubsky, V. G. Makhankov, On the Pulsed Soliton Lifetime in

- Two Classical Relativistic Theory Models, JETP Lett. 24 (1976) 12.
- [42] E. J. Copeland, M. Gleiser, H. R. Muller, Oscillons: Resonant configurations during bubble collapse, Phys. Rev. D 52 (1995) 1920–1933. [arXiv:hep-ph/9503217](#), [doi:10.1103/PhysRevD.52.1920](#).
- [43] G. Fodor, P. Forgacs, P. Grandclement, I. Raecz, Oscillons and Quasi-breathers in the ϕ^4 Klein-Gordon model, Phys. Rev. D 74 (2006) 124003. [arXiv:hep-th/0609023](#), [doi:10.1103/PhysRevD.74.124003](#).
- [44] P.-H. Chavanis, Mass-radius relation of Newtonian self-gravitating Bose-Einstein condensates with short-range interactions. I. Analytical results, Phys. Rev. D84 (4) (Aug. 2011). [arXiv:1103.2050](#), [doi:10.1103/PhysRevD.84.043531](#).
- [45] K. Mukaida, M. Takimoto, M. Yamada, On Longevity of I-ball/Oscillon, JHEP 03 (2017) 122. [arXiv:1612.07750](#), [doi:10.1007/JHEP03\(2017\)122](#).
- [46] H. Zhang, Axion Stars, Symmetry 12 (1) (2019) 25. [arXiv:1810.11473](#), [doi:10.3390/sym12010025](#).
- [47] J. Olle, O. Pujolas, F. Rompineve, Recipes for oscillon longevity, JCAP 09 (2021) 015. [arXiv:2012.13409](#), [doi:10.1088/1475-7516/2021/09/015](#).
- [48] L. Visinelli, Boson stars and oscillatons: A review, Int. J. Mod. Phys. D 30 (15) (2021) 2130006. [arXiv:2109.05481](#), [doi:10.1142/S0218271821300068](#).
- [49] T. Ikeda, C.-M. Yoo, V. Cardoso, Self-gravitating oscillons and new critical behavior, Phys. Rev. D 96 (6) (2017) 064047. [arXiv:1708.01344](#), [doi:10.1103/PhysRevD.96.064047](#).
- [50] G. Fodor, P. Forgacs, M. Mezei, Mass loss and longevity of gravitationally bound oscillating scalar lumps (oscillatons) in D-dimensions, Phys. Rev. D 81 (2010) 064029. [arXiv:0912.5351](#), [doi:10.1103/PhysRevD.81.064029](#).
- [51] C. J. Hogan, M. J. Rees, AXION MINICLUSTERS, Phys. Lett. B 205 (1988) 228–230. [doi:10.1016/0370-2693\(88\)91655-3](#).
- [52] E. W. Kolb, I. I. Tkachev, Axion miniclusters and Bose stars, Phys. Rev. Lett. 71 (1993) 3051–3054. [arXiv:hep-ph/9303313](#), [doi:10.1103/PhysRevLett.71.3051](#).
- [53] E. W. Kolb, I. I. Tkachev, Nonlinear axion dynamics and formation of cosmological pseudosolitons, Phys. Rev. D 49 (1994) 5040–5051. [arXiv:astro-ph/9311037](#), [doi:10.1103/PhysRevD.49.5040](#).
- [54] E. W. Kolb, I. I. Tkachev, Large amplitude isothermal fluctuations and high density dark matter clumps, Phys. Rev. D 50 (1994) 769–773. [arXiv:astro-ph/9403011](#), [doi:10.1103/PhysRevD.50.769](#).
- [55] J. C. Niemeyer, Small-scale structure of fuzzy and axion-like dark matter, arXiv e-prints (12 2019). [arXiv:1912.07064](#), [doi:10.1103/j.pnnp.2020.103787](#).
- [56] B. Barman, N. Bernal, N. Ramberg, L. Visinelli, QCD Axion Kinetic Misalignment without Prejudice, Universe 8 (12) (2022) 634. [arXiv:2111.03677](#), [doi:10.3390/universe8120634](#).
- [57] J. Enander, A. Pargner, T. Schwetz, Axion minicluster power spectrum and mass function, JCAP 12 (2017) 038. [arXiv:1708.04466](#), [doi:10.1088/1475-7516/2017/12/038](#).
- [58] M. Fairbairn, D. J. E. Marsh, J. Quevillon, S. Rozier, Structure formation and microlensing with axion miniclusters, Phys. Rev. D 97 (8) (2018) 083502. [arXiv:1707.03310](#), [doi:10.1103/PhysRevD.97.083502](#).
- [59] A. Arvanitaki, M. Baryakhtar, X. Huang, Discovering the QCD Axion with Black Holes and Gravitational Waves, Phys. Rev. D 91 (8) (2015) 084011. [arXiv:1411.2263](#), [doi:10.1103/PhysRevD.91.084011](#).
- [60] M. J. Stott, D. J. E. Marsh, Black hole spin constraints on the mass spectrum and number of axionlike fields, Phys. Rev. D 98 (8) (2018) 083006. [arXiv:1805.02016](#), [doi:10.1103/PhysRevD.98.083006](#).
- [61] C. Ünal, F. Pacucci, A. Loeb, Properties of ultralight bosons from heavy quasar spins via superradiance, JCAP 05 (2021) 007. [arXiv:2012.12790](#), [doi:10.1088/1475-7516/2021/05/007](#).
- [62] D. F. J. Kimball, K. van Bibber (Eds.), The Search for Ultralight Bosonic Dark Matter, Springer, 2022. [doi:10.1007/978-3-030-95852-7](#).
- [63] S. Chabanier, M. Millea, N. Palanque-Delabrouille, Matter power spectrum: from Ly α forest to CMB scales, Mon. Not. Roy. Astron. Soc. 489 (2) (2019) 2247–2253. [arXiv:1905.08103](#), [doi:10.1093/mnras/stz2310](#).
- [64] T. D. Brandt, Constraints on MACHO Dark Matter from Compact Stellar Systems in Ultra-faint Dwarf Galaxies, Astrophys. J. Lett. 824 (2) (2016) L31. [arXiv:1605.03665](#), [doi:10.3847/2041-8205/824/2/L31](#).
- [65] S. M. Koushiappas, A. Loeb, Dynamics of Dwarf Galaxies Disfavor Stellar-Mass Black Holes as Dark Matter, Phys. Rev. Lett. 119 (4) (2017) 041102. [arXiv:1704.01668](#), [doi:10.1103/PhysRevLett.119.041102](#).
- [66] A. Berlin, R. T. D’Agnolo, S. A. R. Ellis, K. Zhou, Heterodyne broadband detection of axion dark matter, Phys. Rev. D 104 (11) (2021) L111701. [arXiv:2007.15656](#), [doi:10.1103/PhysRevD.104.L111701](#).
- [67] P. W. Graham, S. Hacıömeroğlu, D. E. Kaplan, Z. Omarov, S. Rajendran, Y. K. Semertzidis, Storage ring probes of dark matter and dark energy, Phys. Rev. D 103 (5) (2021) 055010. [arXiv:2005.11867](#), [doi:10.1103/PhysRevD.103.055010](#).
- [68] I. M. Bloch, Y. Hochberg, E. Kuflik, T. Volansky, Axion-like Relics: New Constraints from Old Comagnetometer Data, JHEP 01 (2020) 167. [arXiv:1907.03767](#), [doi:10.1007/JHEP01\(2020\)167](#).
- [69] S. Tulin, H.-B. Yu, Dark Matter Self-interactions and Small Scale Structure, Phys. Rept. 730 (2018) 1–57. [arXiv:1705.02358](#), [doi:10.1016/j.physrep.2017.11.004](#).
- [70] M. Kaplinghat, S. Tulin, H.-B. Yu, Dark Matter Halos as Particle Colliders: Unified Solution to Small-Scale Structure Puzzles from Dwarfs to Clusters, Phys. Rev. Lett. 116 (4) (2016) 041302. [arXiv:1508.03339](#), [doi:10.1103/PhysRevLett.116.041302](#).
- [71] J. S. Bullock, M. Boylan-Kolchin, Small-Scale Challenges to the Λ CDM Paradigm, Ann. Rev. Astron. Astrophys. 55 (2017) 343–387. [arXiv:1707.04256](#), [doi:10.1146/annurev-astro-091916-055313](#).
- [72] J. Eby, K. Mukaida, M. Takimoto, L. C. R. Wijewardhana, M. Yamada, Classical nonrelativistic effective field theory and the role of gravitational interactions, Phys. Rev. D 99 (12) (2019) 123503. [arXiv:1807.09795](#), [doi:10.1103/PhysRevD.99.123503](#).
- [73] H.-Y. Zhang, M. A. Amin, E. J. Copeland, P. M. Saffin, K. D. Lozanov, Classical Decay Rates of Oscillons, JCAP 07 (2020) 055. [arXiv:2004.01202](#), [doi:10.1088/1475-7516/2020/07/055](#).
- [74] R. D. Peccei, H. R. Quinn, CP Conservation in the Presence of Instantons, Phys. Rev. Lett. 38 (1977) 1440–1443. [doi:10.1103/PhysRevLett.38.1440](#).
- [75] R. D. Peccei, H. R. Quinn, Constraints Imposed by CP Conservation in the Presence of Instantons, Phys. Rev. D 16 (1977) 1791–1797. [doi:10.1103/PhysRevD.16.1791](#).
- [76] F. Wilczek, Problem of Strong P and T Invariance in the Presence of Instantons, Phys. Rev. Lett. 40 (1978) 279–282. [doi:10.1103/PhysRevLett.40.279](#).
- [77] S. Weinberg, A New Light Boson?, Phys. Rev. Lett. 40 (1978) 223–226. [doi:10.1103/PhysRevLett.40.223](#).
- [78] L. F. Abbott, P. Sikivie, A Cosmological Bound on the Invisible Axion, Phys. Lett. B 120 (1983) 133–136. [doi:10.1016/0370-2693\(83\)90638-X](#).
- [79] M. Dine, W. Fischler, The Not So Harmless Axion, Phys. Lett. B 120 (1983) 137–141. [doi:10.1016/0370-2693\(83\)90639-1](#).
- [80] J. Preskill, M. B. Wise, F. Wilczek, Cosmology of the Invisible Axion, Phys. Lett. B 120 (1983) 127–132. [doi:10.1016/0370-2693\(83\)90637-8](#).
- [81] P. Auclair, et al., Cosmology with the Laser Interferometer Space Antenna, arXiv e-prints (4 2022). [arXiv:2204.05434](#).
- [82] C.-F. Chang, Y. Cui, Gravitational waves from global cosmic strings and cosmic archaeology, JHEP 03 (2022) 114. [arXiv:2106.09746](#), [doi:10.1007/JHEP03\(2022\)114](#).
- [83] C.-F. Chang, Y. Cui, Stochastic Gravitational Wave Background from Global Cosmic Strings, Phys. Dark Univ. 29 (2020) 100604. [arXiv:1910.04781](#), [doi:10.1016/j.dark.2020.100604](#).
- [84] D. Ellis, D. J. E. Marsh, B. Eggemeier, J. Niemeyer, J. Redondo, K. Dolag, Structure of axion miniclusters, Phys. Rev. D 106 (10) (2022) 103514. [arXiv:2204.13187](#), [doi:10.1103/PhysRevD.106.103514](#).
- [85] H. Xiao, I. Williams, M. McQuinn, Simulations of axion minihalos, Phys. Rev. D 104 (2) (2021) 023515. [arXiv:2101.04177](#), [doi:10.1103/PhysRevD.104.023515](#).
- [86] B. Eggemeier, J. Redondo, K. Dolag, J. C. Niemeyer, A. Vaquero, First Simulations of Axion Minicluster Halos, Phys. Rev. Lett. 125 (4) (2020) 041301. [arXiv:1911.09417](#), [doi:10.1103/PhysRevLett.125.041301](#).

- [87] M. Buschmann, J. W. Foster, B. R. Safdi, Early-Universe Simulations of the Cosmological Axion, Phys. Rev. Lett. 124 (16) (2020) 161103. [arXiv:1906.00967](#), [doi:10.1103/PhysRevLett.124.161103](#).
- [88] C.-F. Chang, Y. Cui, Dynamics of Long-lived Axion Domain Walls and Its Cosmological Implications (9 2023). [arXiv:2309.15920](#).
- [89] R. T. Co, L. J. Hall, K. Harigaya, Axion Kinetic Misalignment Mechanism, Phys. Rev. Lett. 124 (25) (2020) 251802. [arXiv:1910.14152](#), [doi:10.1103/PhysRevLett.124.251802](#).
- [90] C.-F. Chang, Y. Cui, New Perspectives on Axion Misalignment Mechanism, Phys. Rev. D 102 (1) (2020) 015003. [arXiv:1911.11885](#), [doi:10.1103/PhysRevD.102.015003](#).
- [91] Y. Cui, D. Yang, In preparation (In preparation).
- [92] A. Arvanitaki, S. Dimopoulos, M. Galanis, L. Lehner, J. O. Thompson, K. Van Tilburg, Large-misalignment mechanism for the formation of compact axion structures: Signatures from the QCD axion to fuzzy dark matter, Phys. Rev. D 101 (8) (2020) 083014. [arXiv:1909.11665](#), [doi:10.1103/PhysRevD.101.083014](#).
- [93] L. Di Luzio, B. Gavela, P. Quilez, A. Ringwald, Dark matter from an even lighter QCD axion: trapped misalignment, JCAP 10 (2021) 001. [arXiv:2102.01082](#), [doi:10.1088/1475-7516/2021/10/001](#).
- [94] S. Nakagawa, F. Takahashi, M. Yamada, Trapping Effect for QCD Axion Dark Matter, JCAP 05 (2021) 062. [arXiv:2012.13592](#), [doi:10.1088/1475-7516/2021/05/062](#).
- [95] R. T. Co, D. Dunsky, N. Fernandez, A. Ghalsasi, L. J. Hall, K. Harigaya, J. Shelton, Gravitational wave and CMB probes of axion kinination, JHEP 09 (2022) 116. [arXiv:2108.09299](#), [doi:10.1007/JHEP09\(2022\)116](#).
- [96] R. T. Co, K. Harigaya, Axiogenesis, Phys. Rev. Lett. 124 (11) (2020) 111602. [arXiv:1910.02080](#), [doi:10.1103/PhysRevLett.124.111602](#).
- [97] C. Eröncel, G. Servant, ALP dark matter mini-clusters from kinetic fragmentation, JCAP 01 (2023) 009. [arXiv:2207.10111](#), [doi:10.1088/1475-7516/2023/01/009](#).
- [98] A. Loeb, Effective Self-interaction of Dark Matter from Gravitational Scattering, Astrophys. J. Lett. 929 (2) (2022) L24. [arXiv:2203.11962](#), [doi:10.3847/2041-8213/ac6591](#).
- [99] M. Boylan-Kolchin, J. S. Bullock, M. Kaplinghat, Too big to fail? The puzzling darkness of massive Milky Way subhaloes, Mon. Not. R. Astron. Soc. 415 (1) (2011) L40–L44. [arXiv:1103.0007](#), [doi:10.1111/j.1745-3933.2011.01074.x](#).
- [100] M. Boylan-Kolchin, J. S. Bullock, M. Kaplinghat, The Milky Way's bright satellites as an apparent failure of Λ CDM, Mon. Not. R. Astron. Soc. 422 (2) (2012) 1203–1218. [arXiv:1111.2048](#), [doi:10.1111/j.1365-2966.2012.20695.x](#).
- [101] M. Vogelsberger, J. Zavala, A. Loeb, Subhaloes in self-interacting galactic dark matter haloes, Mon. Not. R. Astron. Soc. 423 (4) (2012) 3740–3752. [arXiv:1201.5892](#), [doi:10.1111/j.1365-2966.2012.21182.x](#), [10.1002/asna.19141991009](#).
- [102] M. Rocha, A. H. G. Peter, J. S. Bullock, M. Kaplinghat, S. Garrison-Kimmel, J. Onorbe, L. A. Moustakas, Cosmological Simulations with Self-Interacting Dark Matter I: Constant Density Cores and Substructure, Mon. Not. Roy. Astron. Soc. 430 (2013) 81–104. [arXiv:1208.3025](#), [doi:10.1093/mnras/sts514](#).
- [103] J. Zavala, M. Vogelsberger, M. G. Walker, Constraining self-interacting dark matter with the Milky way's dwarf spheroidals., Mon. Not. R. Astron. Soc. 431 (2013) L20–L24. [arXiv:1211.6426](#), [doi:10.1093/mnras/sls053](#).
- [104] A. H. G. Peter, M. Rocha, J. S. Bullock, M. Kaplinghat, Cosmological Simulations with Self-Interacting Dark Matter II: Halo Shapes vs. Observations, Mon. Not. Roy. Astron. Soc. 430 (2013) 105. [arXiv:1208.3026](#), [doi:10.1093/mnras/sts535](#).
- [105] J. Wolf, G. D. Martinez, J. S. Bullock, M. Kaplinghat, M. Geha, R. R. Muñoz, J. D. Simon, F. F. Avedo, Accurate masses for dispersion-supported galaxies, Mon. Not. R. Astron. Soc. 406 (2) (2010) 1220–1237. [arXiv:0908.2995](#), [doi:10.1111/j.1365-2966.2010.16753.x](#).
- [106] M. Kaplinghat, M. Valli, H.-B. Yu, Too Big To Fail in Light of Gaia, Mon. Not. Roy. Astron. Soc. 490 (1) (2019) 231–242. [arXiv:1904.04939](#), [doi:10.1093/mnras/stz2511](#).
- [107] D. Yang, H.-B. Yu, H. An, Self-Interacting Dark Matter and the Origin of Ultradiffuse Galaxies NGC1052-DF2 and -DF4, Phys. Rev. Lett. 125 (11) (2020) 111105. [arXiv:2002.02102](#), [doi:10.1103/PhysRevLett.125.111105](#).
- [108] D. Yang, H.-B. Yu, Self-interacting dark matter and small-scale gravitational lenses in galaxy clusters, Phys. Rev. D 104 (10) (2021) 103031. [arXiv:2102.02375](#), [doi:10.1103/PhysRevD.104.103031](#).
- [109] H. C. Turner, M. R. Lovell, J. Zavala, M. Vogelsberger, The onset of gravothermal core collapse in velocity-dependent self-interacting dark matter subhaloes, Mon. Not. R. Astron. Soc. 505 (4) (2021) 5327–5339. [arXiv:2010.02924](#), [doi:10.1093/mnras/stab1725](#).
- [110] C. A. Correa, M. Schaller, S. Ploeckinger, N. Anau Montel, C. Weniger, S. Ando, TangoSIDM: Tantalizing models of Self-Interacting Dark Matter, arXiv e-prints (6 2022). [arXiv:2206.11298](#), [doi:10.1093/mnras/stac2830](#).
- [111] D. Yang, E. O. Nadler, H.-B. Yu, Strong Dark Matter Self-interactions Diversify Halo Populations Within and Surrounding the Milky Way, arXiv e-prints (Nov. 2022). [arXiv:2211.13768](#), [doi:10.48550/arXiv.2211.13768](#).
- [112] W. Hu, R. Barkana, A. Gruzinov, Cold and fuzzy dark matter, Phys. Rev. Lett. 85 (2000) 1158–1161. [arXiv:astro-ph/0003365](#), [doi:10.1103/PhysRevLett.85.1158](#).
- [113] R. A. Allsman, et al., MACHO project limits on black hole dark matter in the 1–30 solar mass range, Astrophys. J. Lett. 550 (2001) L169. [arXiv:astro-ph/0011506](#), [doi:10.1086/319636](#).
- [114] P. Tisserand, et al., Limits on the Macho Content of the Galactic Halo from the EROS-2 Survey of the Magellanic Clouds, Astron. Astrophys. 469 (2007) 387–404. [arXiv:astro-ph/0607207](#), [doi:10.1051/0004-6361:20066017](#).
- [115] L. Wyrykowski, J. Skowron, S. Kozłowski, A. Udalski, M. K. Szymański, M. Kubiak, G. Pietrzyński, I. Soszyński, O. Szewczyk, K. Ulaczyk, R. Poleski, P. Tisserand, The OGLE view of microlensing towards the Magellanic Clouds - IV. OGLE-III SMC data and final conclusions on MACHOs, Mon. Not. R. Astron. Soc. 416 (4) (2011) 2949–2961. [arXiv:1106.2925](#), [doi:10.1111/j.1365-2966.2011.19243.x](#).
- [116] T. Blaineau, M. Moniez, C. Afonso, J. N. Albert, R. Ansari, E. Aubourg, C. Coutures, J. F. Glicenstein, B. Goldman, C. Hamadache, T. Lasserre, L. Le Guillou, E. Lesquoy, C. Magneville, J. B. Marquette, et al., New limits from microlensing on Galactic black holes in the mass range $10 M_\odot < M < 1000 M_\odot$, Astron. Astrophys. 664 (2022) A106. [arXiv:2202.13819](#), [doi:10.1051/0004-6361/202243430](#).
- [117] I. Esteban, A. H. G. Peter, S. Y. Kim, Milky Way satellite velocities reveal the Dark Matter power spectrum at small scales, arXiv e-prints (6 2023). [arXiv:2306.04674](#).
- [118] N. Sabti, J. B. Muñoz, D. Blas, New Roads to the Small-scale Universe: Measurements of the Clustering of Matter with the High-redshift UV Galaxy Luminosity Function, Astrophys. J. Lett. 928 (2) (2022) L20. [arXiv:2110.13161](#), [doi:10.3847/2041-8213/ac5e9c](#).
- [119] J. Chluba, D. Grin, CMB spectral distortions from small-scale isocurvature fluctuations, Mon. Not. Roy. Astron. Soc. 434 (2013) 1619–1635. [arXiv:1304.4596](#), [doi:10.1093/mnras/stt1129](#).
- [120] K. K. Rogers, H. V. Peiris, Strong Bound on Canonical Ultralight Axion Dark Matter from the Lyman-Alpha Forest, Phys. Rev. Lett. 126 (7) (2021) 071302. [arXiv:2007.12705](#), [doi:10.1103/PhysRevLett.126.071302](#).
- [121] D. Inman, Y. Ali-Haïmoud, Early structure formation in primordial black hole cosmologies, Phys. Rev. D 100 (8) (2019) 083528. [arXiv:1907.08129](#), [doi:10.1103/PhysRevD.100.083528](#).
- [122] P. Meszaros, The behaviour of point masses in an expanding cosmological substratum., Astron. Astrophys. 37 (2) (1974) 225–228.
- [123] V. Dike, D. Gilman, T. Treu, Strong lensing constraints on primordial black holes as a dark matter candidate, Mon. Not. Roy. Astron. Soc. 522 (4) (2023) 5434–5441. [arXiv:2210.09493](#), [doi:10.1093/mnras/stad1313](#).
- [124] C. Eröncel, R. Sato, G. Servant, P. Sørensen, ALP dark matter from kinetic fragmentation: opening up the parameter window, JCAP 10 (2022) 053. [arXiv:2206.14259](#), [doi:10.1088/1475-7516/2022/10/053](#).
- [125] W. H. Press, P. Schechter, Formation of Galaxies and Clusters of Galaxies by Self-Similar Gravitational Condensation, Astrophys. J. 187 (1974) 425–438. [doi:10.1086/152650](#).
- [126] R. K. Sheth, G. Tormen, Large scale bias and the peak background

- split, Mon. Not. Roy. Astron. Soc. 308 (1999) 119. [arXiv:astro-ph/9901122](#), [doi:10.1046/j.1365-8711.1999.02692.x](#).
- [127] L. Y. A. Yung, R. S. Somerville, S. L. Finkelstein, S. M. Wilkins, J. P. Gardner, Are the ultra-high-redshift galaxies at $z > 10$ surprising in the context of standard galaxy formation models?, arXiv e-prints (Apr. 2023). [arXiv:2304.04348](#), [doi:10.48550/arXiv.2304.04348](#).
- [128] J. Mirocha, S. R. Furlanetto, Balancing the efficiency and stochasticity of star formation with dust extinction in $z \gtrsim 10$ galaxies observed by JWST, Mon. Not. R. Astron. Soc. 519 (1) (2023) 843–853. [arXiv:2208.12826](#), [doi:10.1093/mnras/stac3578](#).
- [129] Y. Gong, B. Yue, Y. Cao, X. Chen, Fuzzy Dark Matter as a Solution to Reconcile the Stellar Mass Density of High- z Massive Galaxies and Reionization History, Astrophys. J. 947 (1) (2023) 28. [arXiv:2209.13757](#), [doi:10.3847/1538-4357/acc109](#).
- [130] G. J. Feldman, R. D. Cousins, A Unified approach to the classical statistical analysis of small signals, Phys. Rev. D 57 (1998) 3873–3889. [arXiv:physics/9711021](#), [doi:10.1103/PhysRevD.57.3873](#).
- [131] J. E. Kim, Weak Interaction Singlet and Strong CP Invariance, Phys. Rev. Lett. 43 (1979) 103. [doi:10.1103/PhysRevLett.43.103](#).
- [132] M. A. Shifman, A. I. Vainshtein, V. I. Zakharov, Can Confinement Ensure Natural CP Invariance of Strong Interactions?, Nucl. Phys. B 166 (1980) 493–506. [doi:10.1016/0550-3213\(80\)90209-6](#).
- [133] M. Dine, W. Fischler, M. Srednicki, A Simple Solution to the Strong CP Problem with a Harmless Axion, Phys. Lett. B 104 (1981) 199–202. [doi:10.1016/0370-2693\(81\)90590-6](#).
- [134] A. R. Zhitnitsky, On Possible Suppression of the Axion Hadron Interactions. (In Russian), Sov. J. Nucl. Phys. 31 (1980) 260.
- [135] J. A. Dror, J. M. Leedom, Cosmological Tension of Ultralight Axion Dark Matter and its Solutions, Phys. Rev. D 102 (11) (2020) 115030. [arXiv:2008.02279](#), [doi:10.1103/PhysRevD.102.115030](#).
- [136] P. Agrawal, J. Fan, M. Reece, L.-T. Wang, Experimental Targets for Photon Couplings of the QCD Axion, JHEP 02 (2018) 006. [arXiv:1709.06085](#), [doi:10.1007/JHEP02\(2018\)006](#).
- [137] P. Agrawal, J. Fan, M. Reece, Clockwork Axions in Cosmology: Is Chromonatural Inflation Chrononatural?, JHEP 10 (2018) 193. [arXiv:1806.09621](#), [doi:10.1007/JHEP10\(2018\)193](#).
- [138] A. Payez, C. Evoli, T. Fischer, M. Giannotti, A. Mirizzi, A. Ringwald, Revisiting the SN1987A gamma-ray limit on ultralight axion-like particles, JCAP 02 (2015) 006. [arXiv:1410.3747](#), [doi:10.1088/1475-7516/2015/02/006](#).
- [139] J. H. Chang, R. Essig, S. D. McDermott, Supernova 1987A Constraints on Sub-GeV Dark Sectors, Millicharged Particles, the QCD Axion, and an Axion-like Particle, JHEP 09 (2018) 051. [arXiv:1803.00993](#), [doi:10.1007/JHEP09\(2018\)051](#).
- [140] M. V. Beznogov, E. Rrapaj, D. Page, S. Reddy, Constraints on Axion-like Particles and Nucleon Pairing in Dense Matter from the Hot Neutron Star in HESS J1731-347, Phys. Rev. C 98 (3) (2018) 035802. [arXiv:1806.07991](#), [doi:10.1103/PhysRevC.98.035802](#).
- [141] K. Hamaguchi, N. Nagata, K. Yanagi, J. Zheng, Limit on the Axion Decay Constant from the Cooling Neutron Star in Cassiopeia A, Phys. Rev. D 98 (10) (2018) 103015. [arXiv:1806.07151](#), [doi:10.1103/PhysRevD.98.103015](#).
- [142] A. Sedrakian, Axion cooling of neutron stars, Phys. Rev. D 93 (6) (2016) 065044. [arXiv:1512.07828](#), [doi:10.1103/PhysRevD.93.065044](#).
- [143] T. Fujita, R. Tazaki, K. Toma, Hunting Axion Dark Matter with Proto-planetary Disk Polarimetry, Phys. Rev. Lett. 122 (19) (2019) 191101. [arXiv:1811.03525](#), [doi:10.1103/PhysRevLett.122.191101](#).
- [144] M. M. Ivanov, Y. Y. Kovalev, M. L. Lister, A. G. Panin, A. B. Pushkarev, T. Savolainen, S. V. Troitsky, Constraining the photon coupling of ultra-light dark-matter axion-like particles by polarization variations of parsec-scale jets in active galaxies, JCAP 02 (2019) 059. [arXiv:1811.10997](#), [doi:10.1088/1475-7516/2019/02/059](#).
- [145] P. W. Graham, D. E. Kaplan, J. Mardon, S. Rajendran, W. A. Terrano, L. Trahms, T. Wilkason, Spin Precession Experiments for Light Axionic Dark Matter, Phys. Rev. D 97 (5) (2018) 055006. [arXiv:1709.07852](#), [doi:10.1103/PhysRevD.97.055006](#).
- [146] T. Liu, G. Smoot, Y. Zhao, Detecting axionlike dark matter with linearly polarized pulsar light, Phys. Rev. D 101 (6) (2020) 063012. [arXiv:1901.10981](#), [doi:10.1103/PhysRevD.101.063012](#).
- [147] V. K. Oikonomou, Flat energy spectrum of primordial gravitational waves versus peaks and the NANOGrav 2023 observation, Phys. Rev. D 108 (4) (2023) 043516. [arXiv:2306.17351](#), [doi:10.1103/PhysRevD.108.043516](#).
- [148] V. K. Oikonomou, Effects of the axion through the Higgs portal on primordial gravitational waves during the electroweak breaking, Phys. Rev. D 107 (6) (2023) 064071. [arXiv:2303.05889](#), [doi:10.1103/PhysRevD.107.064071](#).
- [149] T. Bringmann, P. F. Depta, T. Konstandin, K. Schmidt-Hoberg, C. Tasillo, Does NANOGrav observe a dark sector phase transition?, JCAP 11 (2023) 053. [arXiv:2306.09411](#), [doi:10.1088/1475-7516/2023/11/053](#).
- [150] Y. Gouttenoire, First-Order Phase Transition Interpretation of Pulsar Timing Array Signal Is Consistent with Solar-Mass Black Holes, Phys. Rev. Lett. 131 (17) (2023) 171404. [arXiv:2307.04239](#), [doi:10.1103/PhysRevLett.131.171404](#).
- [151] Y. Gouttenoire, S. Trifinopoulos, G. Valogiannis, M. Vanvlasselaer, Scrutinizing the Primordial Black Holes Interpretation of PTA Gravitational Waves and JWST Early Galaxies (7 2023). [arXiv:2307.01457](#).
- [152] T. Ghosh, A. Ghoshal, H.-K. Guo, F. Hajkarim, S. F. King, K. Sinha, X. Wang, G. White, Did we hear the sound of the Universe boiling? Analysis using the full fluid velocity profiles and NANOGrav 15-year data (7 2023). [arXiv:2307.02259](#).
- [153] A. Chakraborty, P. K. Chanda, K. L. Pandey, S. Das, Formation and Abundance of Late-forming Primordial Black Holes as Dark Matter, Astrophys. J. 932 (2) (2022) 119. [arXiv:2204.09628](#), [doi:10.3847/1538-4357/ac6ddd](#).
- [154] A. Sarkar, S. Das, S. K. Sethi, How Late can the Dark Matter form in our universe?, JCAP 03 (2015) 004. [arXiv:1410.7129](#), [doi:10.1088/1475-7516/2015/03/004](#).
- [155] N. Brouzakis, N. Tetradis, Static configurations of dark energy and dark matter, JCAP 01 (2006) 004. [arXiv:astro-ph/0509755](#), [doi:10.1088/1475-7516/2006/01/004](#).
- [156] M. M. Pieri, S. Bonoli, J. Chaves-Montero, I. Pâris, M. Fumagalli, J. S. Bolton, M. Viel, P. Noterdaeme, J. Miralda-Escudé, N. G. Busca, H. Rahmani, C. Peroux, A. Font-Ribera, S. C. Trager, WEAVE-QSO: A Massive Intergalactic Medium Survey for the William Herschel Telescope, in: C. Reylé, J. Richard, L. Cambresy, M. Deleuil, E. Pécontal, L. Tresse, I. Vauglin (Eds.), SF2A-2016: Proceedings of the Annual meeting of the French Society of Astronomy and Astrophysics, 2016, pp. 259–266. [arXiv:1611.09388](#), [doi:10.48550/arXiv.1611.09388](#).
- [157] N. G. Karaçaylı, P. Martini, J. Guy, C. Ravoux, M. L. A. Karim, E. Armengaud, M. Walther, J. Aguilar, S. Ahlen, S. Bailey, J. Bautista, S. F. Beltran, D. Brooks, L. Cabayol-Garcia, S. Chabanier, et al., Optimal 1D Ly α Forest Power Spectrum Estimation – III. DESI early data, arXiv e-prints (2023) arXiv:2306.06316 [arXiv:2306.06316](#), [doi:10.48550/arXiv.2306.06316](#).
- [158] C. Ravoux, M. L. A. Karim, E. Armengaud, M. Walther, N. Göksel Karaçaylı, P. Martini, J. Guy, J. N. Aguilar, S. Ahlen, S. Bailey, J. Bautista, S. F. Beltran, D. Brooks, L. Cabayol-Garcia, S. Chabanier, et al., The Dark Energy Spectroscopic Instrument: One-dimensional power spectrum from first Lyman- α forest samples with Fast Fourier Transform, arXiv e-prints (2023) arXiv:2306.06311 [arXiv:2306.06311](#), [doi:10.48550/arXiv.2306.06311](#).
- [159] T. Daylan, S. Birrer, Searching for dark matter substructure: a deeper wide-area community survey for Roman, arXiv e-prints (2023) arXiv:2306.12864 [arXiv:2306.12864](#), [doi:10.48550/arXiv.2306.12864](#).